Int. J. Nano Dimens., 15 (1): 72-79, Winter 2024

ORIGINAL ARTICLE

Structure, magnetic, and optical properties of $NiFe_2O_4$ nanoparticle doped on the surface of Carbon nanotube as a substrate

Farshad Taleshi, Reza Moradi, Leila Sohrabi*

Department of Physics, Qaemshahr Branch, Islamic Azad University, Qaemshahr, Iran

Received 24 October 2023, revised 09 December 2023, accepted 26 December 2023, available online 29 December 2023

Abstract

In this research, we investigate the effect of carbon nanotubes (CNTs) as a substrate on the morphology, size, magnetic behavior and band gap energy (E_g) of nickel ferrite nanoparticles. Synthesis of $NiFe_2O_4$ nanoparticles carried out using a direct co-precipitation method in aqueous solution containing carbon nanotubes. The samples were characterized using X-ray diffraction (XRD), scanning electron microscopy (SEM), transmission electron microscopy (TEM), UV-visible Spectrophotometer and vibrating sample magnetometer (VSM). The results showed that using the CNT as a supporter reduced the size and band gap energy of $NiFe_2O_4$ nanoparticles, changed the morphology of the powder from an aggregate state to a filament state and it increased the magnetic saturation properties of nanoparticles.

Keywords: *Band Gap Energy; Carbon Nanotube; Direct Co-Precipitation; Magnetic Saturation; Morphology; Nickel Ferrite Nanoparticle.*

How to cite this article

Taleshi F., Moradi R., Sohrabi L., Structure, magnetic, and optical properties of $NiFe_2O_4$ nanoparticle doped on the surface of Carbon nanotube as a substrate. Int. J. Nano Dimens., 2024; 15(1): 72-79.

INTRODUCTION

Recently, a large number of studies conducted on the various materials at the nanodimension scale. The results of these studies indicated the chemical and physical properties of materials in nano-size have significant difference with the behavior of those materials in bulk size [1, 2]. The increase of surface to volume ratio in the nanoparticles and the appearance of quantum effects are the reason for this behavior [3, 4].

On the other hand, researches in recent years have widely focused on nanoparticles of MFe_2O_4 (M= Fe, Ni, Co, Cu, Zn,...) ferrite. These materials are very important and they have been used in various applications including sensors [5], magnetically guided drug delivery [6], physicochemical and biological applications [7, 8], high-density data storage [9] and ..., because of their interesting thermal, optical, electrical and magnetic properties [10-12].

There are many factors to determining the magnetic properties of nanoparticles, such as the chemical combination, the type and the degree of the lattice weakness, the size and shape of particle, the morphology of powder and the interaction of the nanoparticles with the substrate [13- 15]. The magnetic characteristics of the nanoparticles are controllable with changing the nanoparticle shape, size, their structure and composition. However, these factors cannot be controlled during the process of synthesizing nanoparticles; therefore, the properties of same type nanomaterials can be significantly different.

In order to obtain MFe_2O_4 nanoparticles with preferable physical properties, different synthesis methods have been employed including chemical auto-combustion route [16], sol-gel [17], hydrothermal method [18], conventional ceramic process [19] and RF-sputtering [20] etc. These difference methods bring some changes in the size, morphology, the structure of nanoparticles and their physical and chemical properties [21, 22]. The direct co-precipitation method has been attracting more attention than other common methods due to the lower cost and the possibility to control the size of nanoparticles [23].

* Corresponding Author Email: *reza.moradi.58@gmail.com*

Nickel ferrite ($NiFe_2O_4$) is a cubic spinel structure of soft magnetic material where the Ni^{2+} ion occupies the octahedral sites and the Fe^{3+} ions occupy both the tetrahedral and octahedral sites. It has high magneto crystalline anisotropy, high saturation magnetization and unique magnetic structure. $NiFe_2O_4$ shows different types of magnetic properties like ferromagnetic, paramagnetic and superparamagnetic behavior, which depends on the size and shape of the particles [24].

Nickel ferrite ($NiFe_2O_4$) nanoparticles have many applications in different fields such as biomedical, technological and catalysis applications, microwave devices and ferro-fluid because of their low magnetic coercivity, low saturation magnetization and high electrical resistance [25].

In recent years, carbon nanotubes (CNTs) have generated a various research areas for their individual chemical and physical properties [26]. These materials have widespread applications in the composite and electronics fields, because of their geometric shape. So, CNTs can be used as a substrate for growing the nanoparticles in the preparation of nanocomposite powders. These nanocomposite powders lead to formation of a new group of composite materials with common physical and chemical behaviour of two combined materials [27, 28].

The as-synthesized carbon nanotubes have no ability for growth of $NiFe_2O_4$ nanoparticles. So, functionalization of CNTs surface is necessary for nucleation and growth of nanoparticles. To do this, first the CNTs were oxidized using thermal oxidation at high temperature and then oxidized with mixture of several acids. Thus, the active functional groups such as -COOH, -C=O, -OH placed on the surface of CNTs [27, 29]. These functional groups can act as places for nucleation of metal ions.

In this work, the $NiFe_2O_4$ nanoparticles and $NiFe_2O_4$/CNT nanocomposite are synthesis by a simple direct co-Precipitation method using metal nitrates in aqueous solution as the precursors. The resulted nanoparticles have a crystal sizes about 16.4 nm and 13.1 nm in $NiFe_2O_4$ and $NiFe_2O_4$/CNT, respectively. The samples were characteristic by XRD, SEM and TEM. The magnetic and optical properties of prepared nanoparticles investigate by using a vibrating sample magnetometer (VSM) and UV-visible spectroscopy.

EXPERIMENTS

Materials

In order to prepare the samples, $Ni(NO_3)_2.6H_2O$ (Merck, pure>99%), $FeCl_3.6H_2O$ (Merck, pure>99%), carbon nanotubes CNTs, pure>97%, 20mn<d<30mn, ammonium hydroxide (NH_4OH), sulfuric acid (H_2SO_4) and nitric acid (HNO_3) were used.

Functionalization of CNTs

In order to Functionalization the CNTs surface, the required amount of CNTs sonicated for two hours in a mixed solution of HNO_3/H_2SO_4 (6M). The solution was stirred (1600 rpm) at 80 °C for 2 hours. By passing the solution obtained from filter paper and washing with distilled water until the pH was adjusted to 7. Finally, the functionalized CNTs dried at 120 °C in an oven.

Synthesis of $NiFe_2O_4$ nanoparticles

To prepare the $NiFe_2O_{\backslash 4}$ nanoparticles, first, 0.47 gr of iron chloride and 0.24 gr of nickel nitrate (2 to 1 ratio of Fe^{3+} to Ni^{2+} ions) were dissolved in 20cc distilled water. Then, 25cc of ammonium hydroxide solution added to the above solution during stirring with magnetic stirrer (drop wise) and rotated the solution for half an hour. Then, resulted precipitate was separated from the solution by filtration and washed several times with ethanol and deionized water to reach pH = 7. The final precipitate dried at 120° C in an oven for 4 h. Finally, they were calcinated at 600 °C under (10 % H_2 and 90 % Ar) in a horizontal electric furnace for 2 h.

Synthesis of $NiFe_2O_4$ / CNT nanocomposite

The synthesis process of $NiFe_2O_4$/CNT nanocomposite powder carried out with the same weight ratio of $NiFe_2O_4$ and CNTs, similar to the synthesis of $NiFe_2O_4$ nanoparticles in the presence of carbon nanotubes. We added some of the functionalized CNTs into the solution of iron chloride and nickel nitrate. The synthesis process of nanocomposite continued similar to the synthesis of $NiFe_2O_4$ nanoparticles.

The chemical nature and crystal structure have been determinate of the mean crystalline size of the obtained samples done using X-ray diffractometer (XRD, Philips, pw 1800). The powder morphology was determined using scanning electron microscopy (SEM, Philips, SE, 15kV, 60kx). The calculations of band gap energy

were studied using (UV-Visible Cole Parmer 8852) and the study of magnetic behavior was done by a vibrating magnetometer (VSM, Lake-Shore model 7400).

RESULTS AND DISCUSSION

Fig. 1 shows the X-ray diffraction pattern of $NiFe_2O_4$ nanoparticle powders and $NiFe_2O_4$/CNT nanocomposites. According to the Fig. (1a), (2 2 0), (3 1 1), (2 2 2), (4 0 0), (4 2 2), (5 1 1), (4 4 0) and (5 3 3) peaks at 2θ= 30.47°, 35.81°, 37.47°, 43.42°, 53.6°, 57.37 °, 63.06 °, and 74.57° are depends on the $NiFe_2O_4$ nanoparticles with the Fd3m space group and cubic spinel structure (JCPDF Card No: 10-0325). The $NiFe_2O_4$/CNT nanocomposite has a new peak (002) at 2θ=26° in addition to the peaks related to pure $NiFe_2O_4$ nanoparticles which this peak is due to graphite structure of CNTs (Fig. (1b))[26]. Comparison of the obtained XRD pattern shows that the peak width of $NiFe_2O_4$ nanoparticles increased with the presence of CNTs. Therefore, the average size of particle has decreased. The average crystal size calculated from the highest peaks associated with $NiFe_2O_4$ nanoparticles, using the Scherrer's equation ($D = \frac{K\lambda}{\beta \cos\theta}$), where β is the width of the peak at its half intensity, K is the so-called shape factor, which usually takes a value of about 0.9, and λ is the wavelength of the X-ray source [30]. For pure $NiFe_2O_4$ and $NiFe_2O_4$/CNT nanocomposite powder, the average size of crystals was 16.4 and 13.1 nm, respectively. The results show that the presence of carbon nanotubes in the process of synthesizing of $NiFe_2O_4$ nanoparticles, the size of nanocrystals has significantly decreased.

Fig. 2 shows the SEM images of pure $NiFe_2O_4$ nanoparticles and $NiFe_2O_4$/CNT nanocomposite powder, respectively. As we can see form Fig. 2(a), the pure $NiFe_2O_4$ nanoparticles are stick together and the larger grains created. Such sticking particles can be having a negative effect on the physical behavior of the crystals. However, the presence of carbon nanotube as a substrate significantly decreases the amount of sticking and agglomeration of the nanoparticles in the nanocomposite powder (Fig. (2b)). The image shows all of the nanoparticles are synthesized on the surface of carbon nanotubes with uniform coating and the nano-narrow strands of $NiFe_2O_4$/CNT have been formed. Reducing in the mass of the nanoparticles and forming strands can have a significant effect on the physical behavior of nanoparticles.

Fig. 3 shows TEM images and histograms of

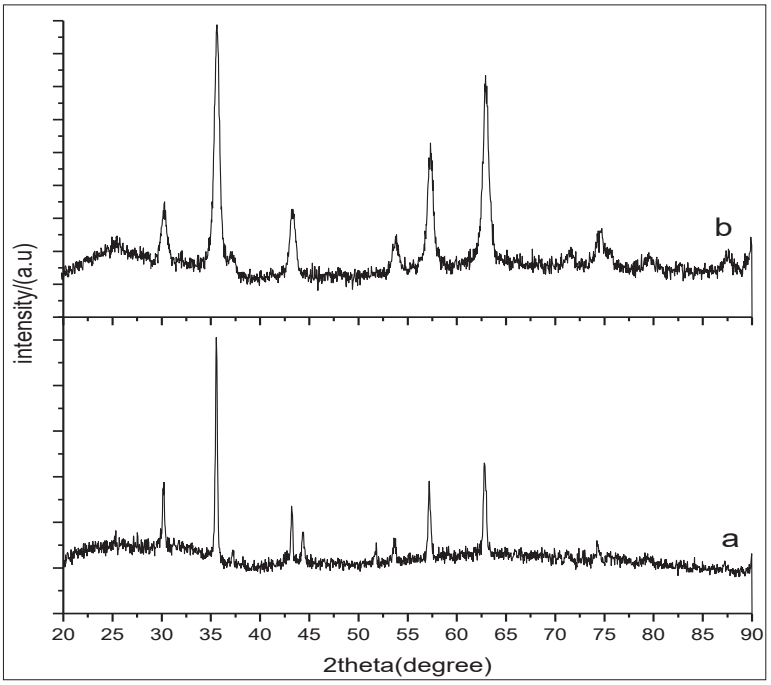

Fig 1: XRD spectra resulting from (a) $NiFe_2O_4$ pure nanoparticles, (b) $NiFe_2O_4$/CNT nanocomposite powder.

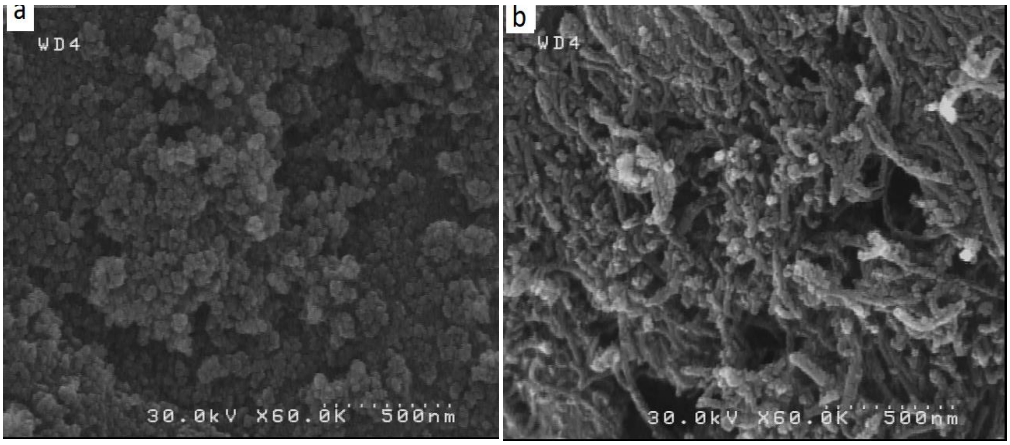

Fig 2: SEM images of (a) pure nanoparticles of $NiFe_2O_4$ and (b) $NiFe_2O_4$/CNT nanocomposite powder calcinated at 600 °C.

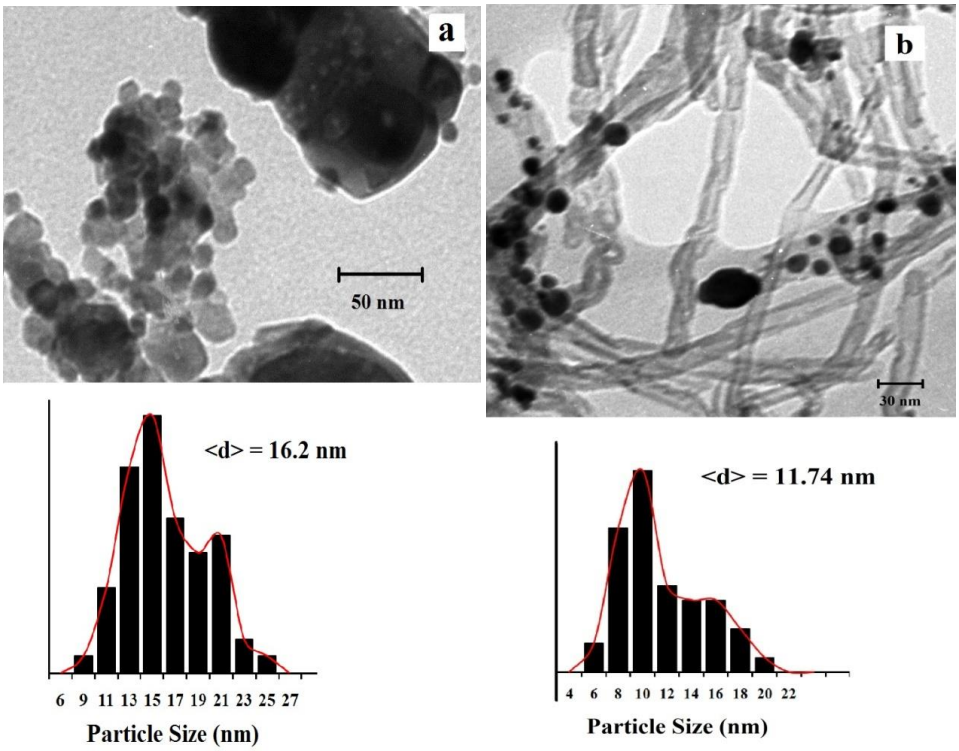

Fig 3: TEM images and histograms of (a) pure nanoparticles of $NiFe_2O_4$ and (b) $NiFe_2O_4$/CNT nanocomposite powder calcinated at 600 °C.

pure $NiFe_2O_4$ nanoparticles and $NiFe_2O_4$/CNT nanocomposite powder, respectively. From Fig. 3(a), we see that calcination at 600 ˚C causes the pure $NiFe_2O_4$ nanoparticles coalescence and grate grains created. However, as shown in Fig. 3(b), the $NiFe_2O_4$ nanoparticles on the surface of CNTs at the same calcination conditions have limited agglomeration and the size of coalesced particles is smaller than if the nanoparticles were alone. The histograms related to nanoparticles size are show in the Fig. 3, and the average size of $NiFe_2O_4$ particles in pure nanoparticles and $NiFe_2O_4$/CNT nanocomposite equals to 16.2 and 11.74 nm, respectively. Therefore, CNTs as an appropriate substrate prevent the $NiFe_2O_4$ nanoparticles from coalescence and the nanoparticles have a uniform distribution of particle size.

To study the effect of presence of carbon

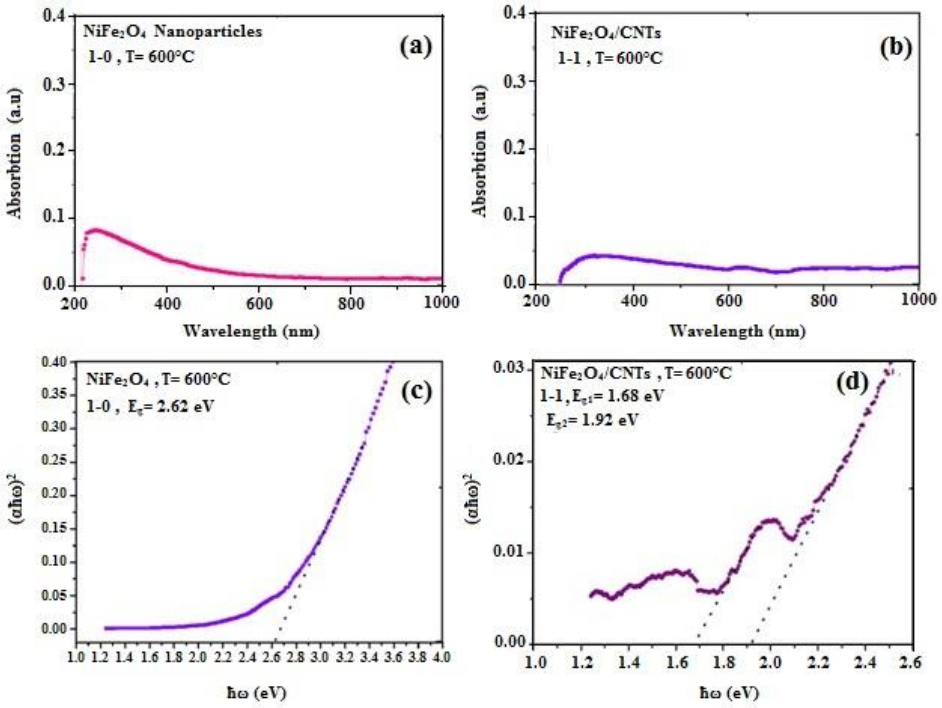

Fig 4: The UV-Visible absorbance spectrum obtained from (a) the pure $NiFe_2O_4$ nanoparticles, (b) the $NiFe_2O_4$/CNT nanocomposite powder and (c, d) plotting the graph $(\alpha\hbar\omega)^2$ according to $(\hbar\omega)$ of the above examples.

nanotubes on the band gap energy of $NiFe_2O_4$ nanoparticles, two UV-Visible powder samples were prepared. The UV-Visible absorption spectrum of $NiFe_2O_4$ nanoparticles and of $NiFe_2O_4$/CNT nanocomposite shown in Fig. 4(a) and 4(b), respectively and their plotting graph for calculation of band gap energy are shown in Fig. 4(c) and 4(d)). We used the Talk relation ($(\alpha h\omega)^n = B(\hbar\omega - E_g)$) to determine the band gap energy of samples [31]. The amount of band gap energy and the type of electronic transition can be determined by plotting the variation diagram $(\alpha\hbar\omega)^n$ in terms of the energy of the incident photon $(\hbar\omega)$ and by extrapolating the linear section of the graphs. The power of n depends on the type of electronic transition in the k space. Its value is n=1, 2, 3, ... for direct transition and n= $\frac{1}{2}, \frac{3}{2}, \frac{5}{2}$, ... for the indirect transition. In this study, the absorption graph for the obtained samples with n =2, shows a better linearity than other potentials. Therefore, the nickel ferrite nanoparticles have a direct dominant electronic transition. By extrapolating the linear section of the graph $(\alpha\hbar\omega)^2$ according to $(\hbar\omega)$, the value of band gap energy for pure $NiFe_2O_4$ nanoparticles is 2.62 eV (Fig 4(c)) and the $NiFe_2O_4$/CNT nanocomposite powder has two different values about 1.68 eV and 1.92 eV (Fig 4(d)).

According to the band gap energy theory, that has an inverse relationship with particle size. Reduction in amount of band gap energy due to the decrease of the size of $NiFe_2O_4$ nanoparticles in the presence of CNTs is contrast with band gap energy theory. Such result can be due to various factors, such as electron interactions between carbon atoms with metal nanoparticles atoms or tension in nanoparticles because of the presence of carbon nanotubes, which results in the formation of energy levels between strips or the quantum size effects due to the very small nature of nanoparticles [27, 28].

To study the effect of carbon nanotube as a substrate on the magnetic behavior of nanoparticles, hysteresis loops obtained from the samples. Fig. 5 shows the VSM spectrum of $NiFe_2O_4$ nanoparticles and $NiFe_2O_4$/CNT nanocomposite powder. According to the computed hysteresis

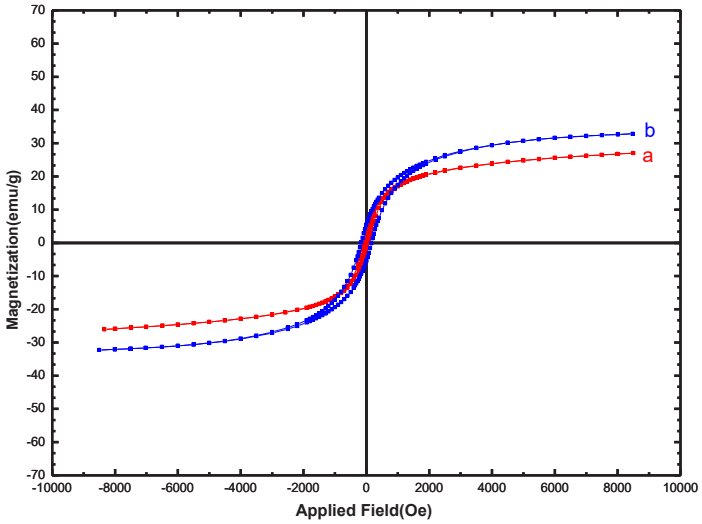

Fig 5: VSM spectrum prepared from (a) $NiFe_2O_4$ nanoparticles and (b) $NiFe_2O_4$/CNT nanocomposite powder.

loop from the pure $NiFe_2O_4$, sample fig. 5(a) and the $NiFe_2O_4$/CNT nanocomposite powder fig. 5(b), their coercivity was 65.13 Oe and 180.65 Oe, their saturation magnetization was 27.03 emu/g and 32.83 emu/g and their magnetic residual was the values of 1.29 emu/g and 3.18 emu/g, respectively. Increasing the saturation magnetization in the presence of carbon nanotubes can be result of changes in the size of nanoparticles, intrinsic tension caused by changes in network parameters or formation of a common bond between nanoparticles with carbon atoms and supercomputing overlap between them. Therefore, magnetism related to the size of the particles and in a certain magnetic field, smaller particles would have more magnetism. In addition, the amounts of force and coercivity directly related to the size of the nanoparticles. By reducing the size of the nanoparticles, the coercivity increased, so that after reaching a maximum value, it tends to zero.

CONCLUSION

In this study, we studied the effects of CNTs as a substrate on the structure, band gap energy and magnetic properties of $NiFe_2O_4$ nanoparticles. $NiFe_2O_4$ nanoparticles powder and $NiFe_2O_4$/CNT nanocomposites have prepared by direct precipitation method in aqueous solution. The results showed that the size of nanoparticles decreased in the presence of carbon nanotubes, while changed the morphology of the powder from aggregation to filament condition. Regarding the linearity of the variation diagram $(\alpha\hbar\omega)^2$, in terms of hω, the dominant transition in $NiFe_2O_4$ nanoparticles is direct type and changing of band gap energy values in the presence CNTs is contrast with the band gap energy theory. The presence of the carbon nanotubes also has the effect of changing the magnetic behavior of $NiFe_2O_4$nanoparticles, which increases the amount of magnetic saturation and magnetic residual content.

ACKNOWLEDGMENTS

The authors would like to acknowledge the Islamic Azad University of Gorgan and Qaemshahr for their financial support of this project.

CONFLICT OF INTEREST

The authors declare no conflicts of interest.

REFERENCES

[1] Wang X., Zhao Z., Qu J., Wang Z., Qiu J., (2010), Fabrication and characterization of magnetic Fe3O4-CNT composites. J. Phys. Chem. Solids. 71: 673-676. https://doi.org/10.1016/j.jpcs.2009.12.063

[2] Sadeghi B., Vahdati R. A. R., (2012), Comparison and SEM-characterization of novel solvents of DNA/carbon nanotube. Appl. Surf. Sci. 258: 3086-3088. https://doi.org/10.1016/j.apsusc.2011.11.042

[3] Gholami-Orimi F., Taleshi F., Biparva P., Karimi-Maleh H., Beitollahi H., Ebrahimi H. R., Shamshiri M., Bagheri H., Fouladgar M., Taherkhani A., (2012), Voltammetric determination of homocysteine using multiwall carbon nanotube paste electrode in the presence of chlorpromazine as a mediator. J. Anal. Methods Chem. 798043; doi:10.1155/2012/902184.

https://doi.org/10.1155/2012/902184
[4] Urquijo J. S., Otálora J. A., Suarez. O. J., (2022), Ferromagnetic resonance of a magnetic particle using the Landau-Lifshitz-Bloch equation. J. Magnetism and Magnetic Materials. 552: 169182. https://doi.org/10.1016/j.jmmm.2022.169182
[5] Patil J. Y., Nadargi D. Y., Gurav J. L., Mulla I. S., Suryavanshi S. S., (2014), Synthesis of glycine combusted NiFe2O4 spinel ferrite: A highly versatile gas sensor. Mat. Let. 124: 144-147. https://doi.org/10.1016/j.matlet.2014.03.051
[6] Long W., Ouyang H., Hu X., Liu M., Zhang X., Feng Y., Wei Y., (2021), State-of-art review on preparation, surface functionalization and biomedical applications of cellulose nanocrystals-based materials. Int. J. Biol. Macromolec. 186: 591-615. https://doi.org/10.1016/j.ijbiomac.2021.07.066
[7] Sivakumar D., Mohamed Rafi M., Sathyaseelan B., Prem Nazeer K. M., Ayisha Begam A. M., (2017). Synthesis and characterization of superparamagnetic Iron Oxide nanoparticles (SPIONs) stabilized by Glucose, Fructose and Sucrose. Int. J. Nano Dimens. 8: 257-264.
[8] Gambhir R. P., Rohiwal S. S., Tiwari A. P., (2022), Multifunctional surface functionalized magnetic iron oxide nanoparticles for biomedical applications: A review. Appl. Surf. Sci. Adv. 11: 100303. https://doi.org/10.1016/j.apsadv.2022.100303
[9] Moradi R., Sebt S. A., Arabi H., (2016), Size controlling of L10-FePt nanoparticles during high temperature annealing on the surface of carbon nanotubes. J. Inorg. Organomet. Polym. 26: 344-352. https://doi.org/10.1007/s10904-015-0322-2
[10] Arabi H., Asnaashari Eivari H., (2014), Applying a suitable route for preparation Fe3O4 nanoparticles by ammonia and investigation of their physical and different magnetic properties Int. J. Nano Dimens. 5: 297-303.
[11] Ghandoor H. E., Zidan H. M., Khalil M. M. H., Ismail M. I. M., (2012), Synthesis and some physical properties of magnetite Fe3O4 nanoparticles. Int. J. Electrochem. Sci. 7: 57734-57745. https://doi.org/10.1016/S1452-3981(23)19655-6
[12] Zhao K., Fang X., Huang Z., Wei G., Zheng A., Zhao Z., (2021), Hydrogen-rich syngas production from chemical looping gasification of lignite by using NiFe2O4 and CuFe2O4 as oxygen carriers. Fuel. 303: 121269. https://doi.org/10.1016/j.fuel.2021.121269
[13] Guo Y., Li S., Yang M., Li H., (2022), A sintering strategy for lithium zinc ferrite with a high saturation magnetization and low ferromagnetic resonance line-width. Ceramics Int. 48: 18067-18073. https://doi.org/10.1016/j.ceramint.2022.02.253
[14] Shen C., Bao Q., Xue W., Sun K., Zhang Z., Jia X., Mei D., Liu C., (2022), Synergistic effect of the metal-support interaction and interfacial oxygen vacancy for CO2 hydrogenation to methanol over Ni/In2O3 catalyst: A theoretical study. J. Energy Chem. 65: 623-629. https://doi.org/10.1016/j.jechem.2021.06.039
[15] Kombaiah K., Vijaya J. J., Kennedy J. L., Bououdina M., Ramalingam R. J., Al-Lohedan H. A., (2017), Comparative investigation on the structural, morphological, optical, and magnetic properties of CoFe2O4 nanoparticles. Ceramics Int. 43: 7682-7689. https://doi.org/10.1016/j.ceramint.2017.03.069
[16] Xu J., Shu R., Shi J., (2022), Synthesis of tetragonal copper-nickel ferrite decorated nitrogen-doped reduced graphene oxide composite as a thin and high-efficiency electromagnetic wave absorber. Colloids and Surf. A: Physicochem. Eng. Aspects. 648: 129411. https://doi.org/10.1016/j.colsurfa.2022.129411
[17] Kombaiah K., Vijaya J. J., Kennedy J. L., Bououdina M., Al-Najar B., (2018), Conventional and microwave combustion synthesis of optomagnetic CuFe2O4 nanoparticles for hyperthermia studies. J. Phys. Chem. Solids. 115: 162-171. https://doi.org/10.1016/j.jpcs.2017.12.024
[18] Singh S., Yadav B. C., Prakash R., Bajaj B., Lee J. R., (2011), Synthesis of nanorods and mixed shaped copper ferrite and their applications as liquefied petroleum gas sensor. Appl. Surf. Sci. 257: 10763-10770. https://doi.org/10.1016/j.apsusc.2011.07.094
[19] Dehno Khalaji A., (2021), Preparation and characterization of PVC/NiFe2O4/Fe2O3 composite: Catalytic activity for synthesis of Arylidene Barbituric acid derivatives. Int. J. Nano Dimens. 12: 37-43.
[20] Sahu B. N., Sahoo S. C., Venkataramani N., Prasad S., Krishnan R., Kostylev M., Stamps R. L., (2013), Magnetic and FMR study on CoFe2O4/ZnFe2O4 bilayers. IEEE Transact. Magnet. 49: 4200-4203. https://doi.org/10.1109/TMAG.2013.2251327
[21] Kukli K., Mikkor M., Šutka A., Kull M., Seemen H., Link J., Stern R., Tamm A., (2020), Behavior of nanocomposite consisting of manganese ferrite particles and atomic layer deposited bismuth oxide chloride film. J. Magnetism and Magnetic Mater. 498: 166167. https://doi.org/10.1016/j.jmmm.2019.166167
[22] Zamani A., Seyed Sadjadi M., Mahjoub A. R., Yousefi M., Farhadyar N., (2020), Synthesis and characterization ZnFe2O4@MnO and MnFe2O4@ZnO magnetic nanocomposites: Investigation of photocatalytic activity for the degradation of Congo Red under visible light irradiation. Int. J. Nano Dimens. 11: 58-73.
[23] Kaur S., Chalotra V. K., Jasrotia R., Bhasin V., Suman., Kumari S., Thakur S., Ahmed J., Mehtab A., Ahmad T., Singh R., Godara S. K., (2022), Spinel nanoferrite (CoFe2O4): The impact of Cr doping on its structural, surface morphology, magnetic, and antibacterial activity traits. Optical Materials. 133: 113026. https://doi.org/10.1016/j.optmat.2022.113026
[24] Godbolea B., Baderab N., Shrivastavac S. B., Jaind D., Sharath Chandrae L. S., Ganesan V., (2013), Synthesis, structural, electrical and magnetic studies of Ni Ferrite nanoparticles. Phys. Procedia. 49: 58-66. https://doi.org/10.1016/j.phpro.2013.10.011
[25] Abdelghani G. M., Al-Zubaidi A. B., Ahmed A. B., (2023), Synthesis, characterization, and study of the influence of energy of irradiation on physical properties and biologic activity of nickel ferrite nanostructures. J. Saudi Chem. Soc. 27: 101623. https://doi.org/10.1016/j.jscs.2023.101623
[26] Baghel P., Sakhiya A. K., Kaushal P., (2022), Ultrafast growth of carbon nanotubes using microwave irradiation: Characterization and its potential applications. Heliyon. 8: e10943. https://doi.org/10.1016/j.heliyon.2022.e10943
[27] Sohrabi L., Taleshi F., Sohrabi R., (2014), Effect of carbon nanotubes support on band gap energy of MgO

nanoparticles. J. Mater. Sci: Mater. Electron. 25: 4110-4114. https://doi.org/10.1007/s10854-014-2136-3

[28] Maity D., Kumar R. T. R., (2019), Highly sensitive amperometric detection of glutamate by glutamic oxidase immobilized Pt nanoparticle decorated multiwalled carbon nanotubes (MWCNTs)/polypyrrole composite. Biosensors and Bioelectronics. 130: 307-314. https://doi.org/10.1016/j.bios.2019.02.001

[29] Avile's F., Cauich-Rodrı'guez J. V., Moo-Tah L., May-Pat A., (2009), Vargas-Coronado R., evaluation of mild acid oxidation treatments for MWCNT functionalization. Carbon. 47: 2970-2975. https://doi.org/10.1016/j.carbon.2009.06.044

[30] Venkateswarlu K., Chandra Bose A., Rameshbabu N., (2010), X-ray peakbroadening studies of nanocrystalline hydroxyapatite by Williumson-Hall analysis. Phys. B. 405: 4256-4261. https://doi.org/10.1016/j.physb.2010.07.020

[31] Tauc J. (1974). Amorphous and Liquid Semiconductors. Plenum Press, New York. https://doi.org/10.1007/978-1-4615-8705-7